古 脊 椎 动 物 学 报
VERTEBRATA PALASIATICA

DOI: 10.19615/j.cnki.2096-9899.241225

CSTR: 32090.14.j.cnki.2096-9899.241225

Cranial anatomy of *Anchiornis huxleyi* (Theropoda: Paraves) sheds new light on bird skull evolution

WANG Min[1] WANG Xiao-Li[2,3] ZHENG Xiao-Ting[2,3] ZHOU Zhong-He[1]

(1 *Key Laboratory of Vertebrate Evolution and Human Origins of Chinese Academy of Sciences*, *Institute of Vertebrate Paleontology and Paleoanthropology*, *Chinese Academy of Sciences* Beijing 100044 wangmin@ivpp.ac.cn)
(3 *Institute of Geology and Paleontology, Linyi University* Linyi, Shandong 276005)
(2 *Shandong Tianyu Museum of Nature* Pingyi, Shandong 273300)

Abstract The origin of birds from theropod dinosaurs, by any measures, is the most eye-catching evolutionary transition in the history of life, which encompasses numerous extensive morphological and biological changes. Compared to postcranium, little progress has been made regarding the evolutionary assemblage of the birds' skull, because of few detailed early records of cranial materials of stem lineages. *Anchiornis* is the oldest known record of the Paraves (~160 Ma), the most inclusive clade that contains all living birds but not *Caudipteryx* or *Epidexipteryx*. With hundreds of known specimens, *Anchiornis* constitutes an ideal taxon for investigating morphological modifications across the theropod-bird transition, but its cranial morphology remains enigmatic. Here we present in-depth description of the cranial morphology of *Anchiornis* based on three-dimensional reconstruction of a well-preserved specimen, including elements from the temporal and palatal regions that are poorly recognized previously. Our study shows that *Anchiornis* retains the plesiomorphic dinosaurian condition in having a diapsid akinetic skull. The mixture of cranial characters, shared with dromaeosaurids, troodontids, and stemward avialans, present in *Anchiornis* demonstrates the complex history of early avialan cranial evolution.

Key words *Anchiornis*, Avialae, cranium, kinesis, palatine, squamosal

Citation Wang M, Wang X L, Zheng X T et al., in press. Cranial anatomy of *Anchiornis huxleyi* (Theropoda: Paraves) sheds new light on bird skull evolutiona. Vertebrata PalAsiatica. DOI: 10.19615/j.cnki.2096-9899.241225

1 Introduction

Anchiornis is the first known Jurassic paravian that is stratigraphically older than *Archaeopteryx*, and its discovery has effectively reconciled the "temporal paradox"—a

国家自然科学基金杰出青年基金(批准号：42225201)、中国科学院前沿科学重点研究计划从"0到1"原始创新十年择优项目(编号：ZDBS-LY-DQC002), 新基石科学基金会所设立的科学探索奖，和山东省泰山学者工程(编号：Ts20190954)资助。

收稿日期：2024-10-29

problem that has been used against the theropod origin of birds (Zhou, 2004; Xu et al., 2014; Wang and Zhou, 2017; Rauhut and Foth, 2020). Over the last decade, several Jurassic paravians have been found, and most of them were unearthed from the Middle–Late Jurassic Yanliao biota, northeast China (Hu et al., 2009; Xu et al., 2011; Godefroit et al., 2013), where all *Anchiornis* specimens have been collected (Pei et al., 2017a; Zhou and Wang, 2017). These fossils have significantly filled the morphological gap between non-avialan and avialan paravian bauplan, and dragged back the initial appearances of many characteristic features of the crown groups to the deep phylogeny of the Avialae (Xu et al., 2014; Brusatte et al., 2015). However, systematic relationships among earliest diverging paravians have been clouded by exceedingly rare fossil records and poor preservation (Agnolin and Novas, 2013; Rauhut and Foth, 2020). Specifically, the known Jurassic paravians are preserved in two dimensions, which hampers examination of morphology of skeletal elements, particularly the skull which consists of delicate bones and bears phylogenetic and functional information. Here we provide a detailed morphological description and comparison of the skull of *Anchiornis huxleyi* based on x-ray CT scanning data. Our study not only revises previously misinterpreted cranial features but also documents previously unrecorded morphologies, which help advances in better understanding the early-diverging paravian cranial evolution.

2 Materials and methods

CT imaging In order to optimize the resolution of computed tomography (CT) scanning, the skull of *Anchiornis huxleyi* (STM 0-47) and the associated anterior cervical vertebrae have been extracted from the slab. The skull was scanned using the industrial CT scanner Phoenix v-tome-x at the Institute of Vertebrate Paleontology and Paleoanthropology, Chinese Academy of Sciences (IVPP) in Beijing (Figs. 1–3). The experiment was conducted using beam energy of 130 kV and a flux of 100 μA at a resolution of 12.163 μm. The obtained scanned images were imported into Avizo (v. 9.2.0) for digital segmentation, rendering and reconstruction.

Phylogenetic analysis In order to explore the phylogenetic position of *Anchiornis huxleyi* in light of the revised cranial morphology, phylogenetic analysis was performed using the latest version of the Theropod Working Group matrix (Brusatte et al., 2014; Turner et al., 2021; Xu et al., 2023). All the cranial characters of *A. huxleyi* have been checked and revised based on present study, but character scorings of the postcranial regions remained unchanged. The phylogenetic analysis was conducted using the TNT v. 1.5 software package (Goloboff and Catalano, 2016), with same settings as in previous study (Xu et al., 2023). Specifically, all characters were equally weighted under parsimony. The New Technology search method, with sectorial search, ratchet, tree drifted and tree fusion, was applied to perform a heuristic tree

search, with the shortest tree found in 20 replicates to uncover as many tree island as possible. Bootstrap and Bremer values were calculated as the supporting indices. The absolute bootstrap values were calculated suing 1000 replicates with the same setting as in the primary search. Bremer values were calculated using the script embedded in TNT.

Fig. 1 Photograph of *Anchiornis huxleyi* (STM 0-47) from Jianchang, Liaoning
Scale bar = 10 cm

Fig. 2 Photograph of the skull of *Anchiornis huxleyi* (STM 0-47) from Jianchang, Liaoning
Scale bar = 10 mm

Institutional abbreviations BMNHC, Beijing Museum of Natural History, Beijing, China; IVPP, Institute of Vertebrate Paleontology and Paleoanthropology, Chinese Academy of Sciences, Beijing, China; LPM, Liaoning Plaeontological Museum, Shenyang, China; PKUP, Peking University Paleontological Museum, Beijing, China; STM, Shandong Tianyu Museum of Nature, Shandong, China.

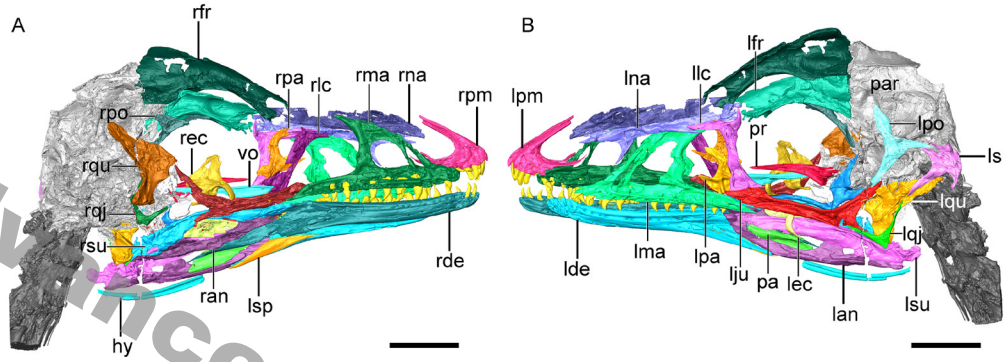

Fig. 3 Digital reconstitution of the skull of *Anchiornis huxleyi* (STM 0-47) from Jianchang, Liaoning in right (A) and left (B) lateral views showing cranial anatomy
Abbreviations: hy. hyoid; lan. left angular; lde. left dentary; lec. left ectopterygoid; lfr. left frontal; lju. left jugal; llc. left lacrimal; lma. left maxilla; lna. left nasal; lpa. left palatine; lpm. left premaxilla; lpo. left postorbital; lqj. left quadratojugal; lqu. left quadrate; ls. left squamosal; lsp. left splenial; lsu. left surangular; pa. prearticular; par. parietal; pr. parasphenoid rostrum; ran. right angular; rde. right dentary; rec. right ectopterygoid; rfr. right frontal; rlc. right lacrimal; rma. right maxilla; rna. right nasal; rpa. right palatine; rpm. right premaxilla; rpo. right postorbital; rqj. right quadratojugal; rqu. right quadrate; rsu. right surangular; vo. vomer. Scale bars = 10 mm

3 Description

As in early-diverging paravians (Ostrom, 1969; Makovicky and Norell, 2004; Turner et al., 2012; Wang and Zhou, 2017), the premaxillae of *Anchiornis* are unfused (Fig. 4A). The rostrum is more pointed than in most deinonychosaurs (Norell and Makovicky, 2004), comparable to that of *Archaeopteryx* (Elżanowski and Wellnhofer, 1996). The rostral tip curves anterodorsally, in stark contrast to the straight condition that is present in other paravians (Xu et al., 2011; Sullivan and Xu, 2017), including *Sinovenator* (Xu et al., 2002), *Dromaeosaurus* (Currie, 1995), and *Archaeopteryx* (Elżanowski and Wellnhofer, 1996). In contrast, the rostral end bends ventrally in *Sapeornis* and *Jeholornis* (Hu et al., 2019, 2022). Like *Archaeopteryx* and other non-avialan paravians (Norell et al., 2006; Tsuihiji et al., 2014; Xu et al., 2015), the nasal processes are short, rather than being elongate and contacting the frontal as in confuciusornithids and some ornithothoracines (O'Connor and Chiappe, 2011; Wang et al., 2019, 2021, 2022). The maxillary process curves posterodorsally with a tapering end (Fig.

3A), contrasting with the blunt form seen in other paravians such as *Archaeopteryx* and *Sinovenator* (Xu et al., 2002; Mayr et al., 2005). The maxilla is probably excluded from the participation in the margin of the external naris, given the length of the maxillary process of the premaxilla and the ventral process of the nasal. This condition present in *Anchiornis* is widely distributed in dromaeosaurids (Norell and Makovicky, 2004; Xu et al., 2015), but absent in stemward avialans (e.g., *Archaeopteryx*, enantiornithines) and troodontids such as *Byronosaurus*, *Almas*, and *Sinovenator* (Xu et al., 2002; Makovicky et al., 2003; Mayr et al., 2005; O'Connor and Chiappe, 2011; Pei et al., 2017b; Wang et al., 2021). As in early-diverging avialans and some troodontids such as *Mei* (Mayr et al., 2005; Turner et al., 2012; Pei et al., 2017a; Wang et al., 2021), the external naris extends posteriorly beyond the anterior margin of the antorbital fossa in *Anchiornis*, opposite to the condition seen in dromaeosaurids and some troodontids such as *Byronosaurus* (Makovicky et al., 2003; Makovicky and Norell, 2004; Norell and Makovicky, 2004).

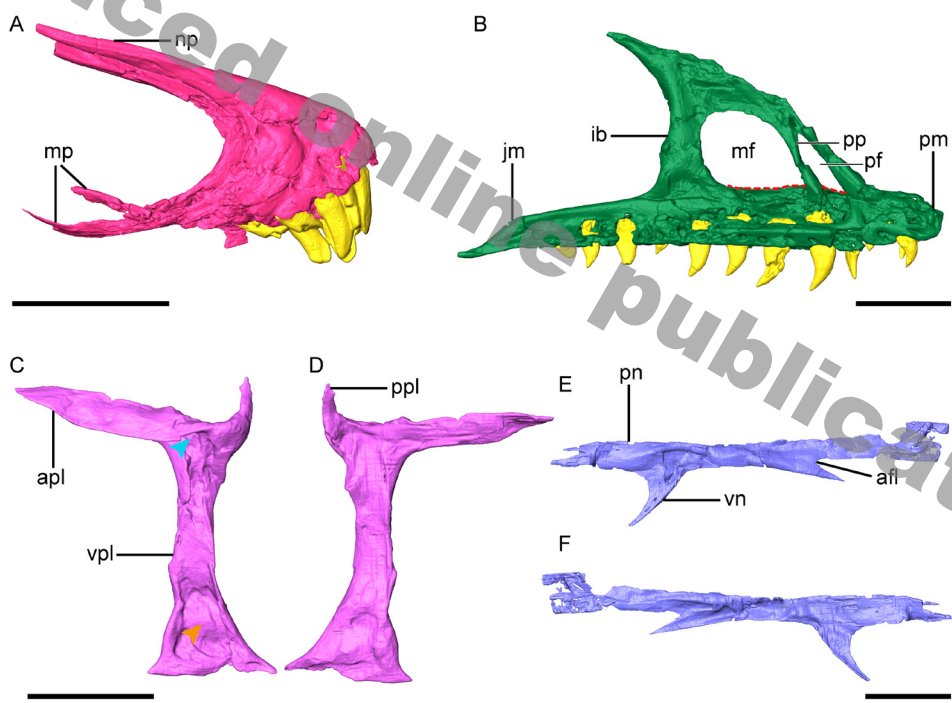

Fig. 4 Anatomy of facial elements of *Anchiornis huxleyi* (STM 0-47) from Jianchang, Liaoning

Digital reconstruction of the left premaxilla (A), right maxilla (B), left lacrimal (C, D), and left nasal (E, F) A–C, E. lateral views; D, F. medial views. The blue arrowhead indicates the recess at the juncture of the anterior and ventral processes, and the orange arrowhead denotes the lateral fossa on the ventral process Abbreviations: afl. articular facet for lacrimal; apl. anterior process of lacrimal; ib. interfenestral bar; jm. jugal process of maxilla; mf. maxillary fenestra; mp. maxillary process; np. nasal process; pf. promaxillary fenestra; pm. premaxillary process; pn. premaxillary process of nasal; pp. promaxillary pila; ppl. posterior process of lacrimal; vn. ventral process of nasal; vpl. ventral process of lacrimal. Scale bars = 5 mm

As in deinonychosaurs (Ostrom, 1969; Xu and Wu, 2001; Xu et al., 2015), but unlike stemward avialans such as *Archaeopteryx* (Mayr et al., 2005; Wang et al., 2021; Hu et al., 2022), the anterior process of the maxilla is substantially shorter than its posterior counterpart (Fig. 4A). The posterior process terminates with a sharply tapering end, contrasting with the blunt form that is present in troodontids (Makovicky and Norell, 2004; Tsuihiji et al., 2014), dromaeosaurids (Norell and Makovicky, 2004), and early avialans (O'Connor and Chiappe, 2011; Rauhut et al., 2018; Wang et al., 2019). The lateral surface of the maxilla is concave. The dorsal process of the maxilla is inset from the labial surface of the maxilla, and it is largely occupied by the antorbital fossa (Fig. 4A). As in dromaeosaurids and basal troodontids (e.g., *Sinovenator*; Xu et al., 2002, 2015; Norell and Makovicky, 2004), both maxillary and promaxillary fenestrae are laterally exposed (Fig. 4A). In contrast, the promaxillary fenestra is absent in later-diverging troodontids (e.g., *Zanabazar* and *Saurornithoides*; Norell et al., 2009), and avialans except for *Archaeopteryx* (Rauhut et al., 2018; Wang et al., 2021; Li et al., 2023). Our digital reconstruction shows that both fenestrae differ greatly from previous description (Hu et al., 2009; Pei et al., 2017a). The promaxillary fenestra is elliptical with the long axis posterodorsally oriented, rather than being rounded as depicted in Hu et al. (2009). As in *Sinovenator* (Xu et al., 2002), the promaxillary fenestra is level with, rather than being more ventrally positioned than, the maxillary fenestra (contrary to Pei et al., 2017a). The promaxillary fenestra is proportionately much larger than in dromaeosaurids (Norell and Makovicky, 2004; Xu et al., 2015) and *Archaeopteryx*, in which the fenestra is more ventrally located relative to the maxillary fenestra (Xu and Wu, 2001; Norell et al., 2006; Rauhut et al., 2018). The promaxillary and maxillary fenestrae are separated by the rod-like, posterodorsally oriented promaxillary pila (Fig. 4A), contrasting with the anteroposteriorly broad form that is present in some troodontids such as *Sinovenator* (Xu et al., 2002; Makovicky et al., 2003; Pei et al., 2017b), and most dromaeosaurids (e.g., *Bambiraptor*, *Velociraptor*, and *Sinornithosaurus*; Barsbold and Osmólska, 1999; Xu and Wu, 2001; Norell and Makovicky, 2004). The maxillary fenestra has a straight ventral margin and its anteroventral corner is constricted, rather than being rounded as described previously (Hu et al., 2009; Pei et al., 2017a). It extends as far ventrally as the antorbital fenestra, unlike in dromaeosaurids in which it is more dorsally located (Norell and Makovicky, 2004). As in other troodontids except for *Byronosaurus* (Makovicky et al., 2003; Norell et al., 2009), the interfenestral bar is inset from the lateral surface of the maxilla (Fig. 4A). An interfenestral canal of the kind present in *Byronosaurus* is absent in *Anchiornis* (Makovicky et al., 2003).

The T-shaped lacrimal is distinguishable from other paravians (Fig. 4C, D). Specifically, the anterior process is less than half the length of the ventral process, proportionately much shorter than in early avialans (e.g., *Archaeopteryx*, *Aurornis*) and dromaeosaurids (Mayr et al., 2005; Godefroit et al., 2013; Rauhut et al., 2018); whereas, the former is subequal to or

longer than the latter in some troodontids such as *Jianianhualong*, *Gobivenator*, and *Almas* (Tsuihiji et al., 2014; Pei et al., 2017b; Xu et al., 2017). As in troodontids (Makovicky et al., 2003), dromaeosaurids (Norell et al., 2006), and *Archaeopteryx* (Rauhut et al., 2018), a recess is developed at the juncture of the three processes (Fig. 4C). Pei et al. (2017a) described a recess on the ventral surface of the anterior process, which is absent in STM 0-47. This recess is absent in crownward avialans such as enantiornithines (Wang et al., 2022; Wang, 2023). The recess is overhung by the dorsoventrally compressed anterior process. The short posterior process deflects dorsally and forms a L-shaped dorsal margin with the anterior process (Fig. 4D). In contrast, the posterior process is straight and extends posterodorsally in other paravians (Norell et al., 2006; O'Connor and Chiappe, 2011; Tsuihiji et al., 2014; Rauhut et al., 2018), and similar morphology was erroneously adopted for *Anchiornis huxleyi* (Hu et al., 2009; Pei et al., 2017a). Reexamination of previously described specimens of *A. huxleyi* reveals that the posterior process is either heavily compressed (BMNHC PH804, PH823 in Pei et al., 2017a) or overlain by other elements (LPM-B00169 in Hu et al., 2019; PKUP V1068, BMNHC PH822 in Pei et al., 2017a), making the original description problematic. The lacrimal lacks a pneumatic fossa between the posterior and ventral processes, but this structure is widely distributed in deinonychosaurs and some early-diverging avialans such as *Jeholornis* and *Parabohaiornis* (Norell et al., 2009; Tsuihiji et al., 2014; Xu et al., 2015; Hu et al., 2022; Wang, 2023). As in *Archaeopteryx* and dromaeosaurids (Norell and Makovicky, 2004; Rauhut et al., 2018), the robust ventral process is expanded anteroposteriorly at the ventral end, forming a large articular facet for the jugal. In contrast, the ventral end tapers or it is blunt in some troodontids such as *Sinovenator* and *Jianianhualong* (Xu et al., 2017; Yin et al., 2018), and some stemward avialans (Hu et al., 2022; Wang et al., 2022; Wang, 2023). Like *Archaeopteryx* and dromaeosaurids (Norell and Makovicky, 2004; Rauhut et al., 2018), the ventral process is perpendicular to the anterior process, rather than curving anteroventrally as in some troodontids such as *Gobivenator*, *Saurornithoides*, and *Byronosaurus* (Makovicky et al., 2003; Norell et al., 2009; Tsuihiji et al., 2014). The lateral surface of the ventral process is deeply excavated by a fossa along its ventral third (Fig. 4C), a unique feature otherwise unknown among early-diverging paravians (Norell and Makovicky, 2004; O'Connor and Chiappe, 2011; Rauhut et al., 2018; Yin et al., 2018; Wang et al., 2021).

The left nasal is relatively well-preserved which compensates anatomical information that remains elusive so far (Fig. 4E, F; Hu et al., 2009; Xu et al., 2009; Pei et al., 2017a). As in other troodontids (Makovicky et al., 2003; Pei et al., 2017b), the bone is proportionately much slender than in some early avialans such as *Archaeopteryx*, *Sapeornis*, and some enantiornithines (O'Connor and Chiappe, 2011; Rauhut et al., 2018; Hu et al., 2019). The triangular ventral process is stout and longer than previously appreciated (Hu et al., 2009).

The premaxillary process is anteriorly forked with a longer ventral and shorter dorsal branches (Fig. 4E). Similar morphology is otherwise unknown among Mesozoic paravians (Makovicky and Norell, 2004; Norell and Makovicky, 2004; O'Connor and Chiappe, 2011; Wang et al., 2021). The nasal has a forked posterior end to articulate with the lacrimal, contrasting with the simply tapering or blunt form present in most other early paravians (Norell et al., 2009; Xu et al., 2015; Rauhut et al., 2018; Wang et al., 2019).

As in troodontids and stemward avialans, the T-shaped postorbital has three slender processes (Fig. 5A; Tsuihiji et al., 2014; Rauhut et al., 2018; Yin et al., 2018; Wang et al., 2021), contrasting with the broad form in dromaeosaurids (Currie, 1995; Norell and Makovicky, 2004). The jugal and frontal processes are subequal in length, contrasting with the large difference that is present in early-diverging troodontids and some stemward avialans (Tsuihiji et al., 2014; Rauhut et al., 2018; Yin et al., 2018; Wang et al., 2021). Specifically, the former is >1.5 times longer than the latter in *Almas*, *Sinovenator*, *Archaeopteryx*, and *Yuanchuavis*; whereas, in dromaeosaurid the three processes are of equal length (Hu et al., 2009; Pei et al., 2017b; Rauhut et al., 2018; Yin et al., 2018; Wang et al., 2022). The articulated right postorbital and jugal show that a complete postorbital bar is present in *Anchiornis* (Fig. 3B), as in other non-avialan theropods and stemward avialans (Currie, 1995; Weishampel et al., 2004; Wang et al., 2021).

The squamosal is an enigmatic element that is rarely well-preserved in Jurassic paravians, which to our knowledge is preserved intact in no other reported specimens of *Anchiornis huxleyi* (Hu et al., 2009; Pei et al., 2017a). The squamosal shares features with *Archaeopteryx* and *Deinonychus* in having a postorbital process that is anteriorly deeply forked, an elongate quadratojugal process, and a paroccipital process that is flexed ventrally (Fig. 5B, C; Ostrom, 1969; Elżanowski and Wellnhofer, 1996). In contrast, the postorbital process is not forked in some stemward avialans such as *Jeholornis* and enantiornithines (Wang et al., 2021; Hu et al., 2022); and the paroccipital process protrudes posterolaterally in some dromaeosaurids (e.g., *Linheraptor*) and enantiornithines such as *Parabohaiornis* and *Yuanchuavis* (Xu et al., 2015; Wang et al., 2022; Wang, 2023). The quadratojugal process projects less anteriorly than in *Archaeopteryx* and *Deinonychus* (Ostrom, 1969; Elżanowski and Wellnhofer, 1996), and it forms a right angle with the postorbital process (Fig. 5B). The preserved left squamosal and quadratojugal approach to each other but not contacting directly (Fig. 3B), which we interpret as a preservational artifact. Because the left squamosal has been posteriorly displaced and thus offset from the postorbital, resulting in the short distance between the squamosal and quadratojugal. Therefore, we suggest that the squamosal contacts the quadratojugal, demonstrating that *Anchiornis* still retained the archosaurian plesiomorphy of having the quadrate foramen fully separated from the infratemporal fenestra. Pei et al. (2017a) argued that *Anchiornis* probably lacked the squamosal-

quadratojugal articulation as in some troodontids, including *Almas*, *Mei*, and *Sinovenator* (Pei et al., 2017b; Yin et al., 2018). Our study points it out that some of these interpretations should be reconsidered given the poor preservation of these paravians.

Our three-dimensional reconstruction of the jugal (Fig. 5D, E) reveals morphologies that are largely consistent with previous study (Pei et al., 2017a). The bone is much slender than in most non-avialan theropods. The straight suborbital process is excavated laterally (Fig. 5E), a feature absents in early avialans (e.g., *Jeholornis*, confuciusornithids) and some troodontids (e.g., *Almas* and *Sinovenator*; Pei et al., 2017b; Yin et al., 2018). The previous study recognized a longitudinal groove along the dorsomedial margin of the jugal as a diagnostic character of *Anchiornis* (Hu et al., 2009). However, our three-dimensional reconstruction of both jugals shows no sign of this groove (Fig. 5D), indicating that this feature cannot be considered valid diagnostic character. As in many paravians including *Archaeopteryx* (Norell and Makovicky, 2004; Mayr et al., 2005; Wang and Hu, 2017), the jugal tapers anteriorly, rather than being forked (contrary to Turner et al., 2012); whereas, an anteriorly forked jugal is present in some troodontids such as *Gobivenator*,

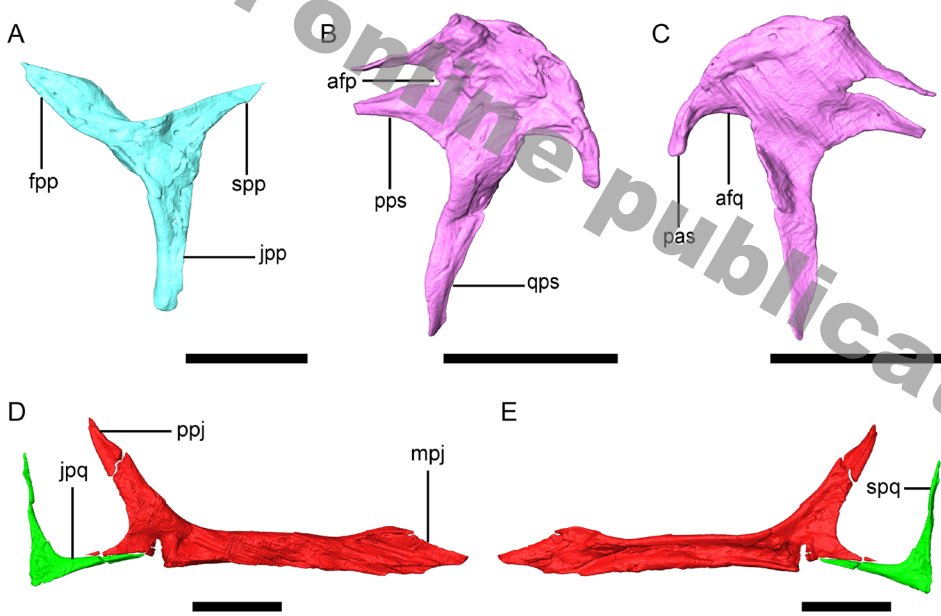

Fig. 5 Anatomy of the temporal elements of *Anchiornis huxleyi* (STM 0-47) from Jianchang, Liaoning

Digital reconstruction of the left postorbital (A), left squamosal (B, C), and right jugal and quadratojugal (D, E)

A, B, E. lateral views; C, D. medial views

Abbreviations: afp. articular facet for postorbital; afq. articular facet for quadrate; fpp. frontal process of postorbital; jpp. jugal process of postorbital; jpq. jugal process of quadratojugal; mpj. maxillary process of jugal; pas. parietal process of squamosal; ppj. postorbital process of jugal; pps. postorbital process of squamosal; qps. quadratojugal process of squamosal; spp. squamosal process of postorbital; spq. squamosal process of quadratojugal. Scale bars = 5 mm

Jinfengopteryx, and *Almas* (Tsuihiji et al., 2014; Pei et al., 2017b). The postorbital process projects posterodorsally and lacks the corneal process on the posterior margin that is present in *Archaeopteryx* and the enantiornithine IVPP V17901 (Wang and Hu, 2017; Wang et al., 2021). The posterior margin between the postorbital and quadratojugal processes is rounded, contrasting with the deeply notched condition present in *Archaeopteryx* (Rauhut et al., 2018). The quadratojugal process lacks the posterior incisure that is present in many non-avialan theropods such as *Sinovenator* and some dromaeosaurids (Xu et al., 2015; Sullivan and Xu, 2017; Yin et al., 2018).

Little was known about the morphology of the quadratojugal in *Anchiornis*, and this element is exquisitely preserved here (Fig. 5D, E). As in troodontids and early avialans (Wang and Hu, 2017; Yin et al., 2018), the bone is L-shaped, without the posterior process that is present in non-avialan theropods including dromaeosaurids (Turner et al., 2012; Sullivan and Xu, 2017). Hu et al. (2009) reconstructed a V-shaped quadratojugal with a prominent posterior end in *Anchiornis*, which resembles the condition of some dromaeosaurids such as *Linheraptor*. Our study shows that this reconstruction is inaccurate. The squamosal and jugal processes are subequal in length, and together they form a right angle. The squamosal process extends as far dorsally as the postorbital process of the jugal (Fig. 5D). In contrast, the postorbital process of the jugal extends more dorsally in early-diverging avialans (e.g., *Archaeopteryx*, *Jeholornis*; Wang and Hu, 2017), and troodontids such as *Mei*, *Sinovenator*, and *Gobivenator* (Tsuihiji et al., 2014; Yin et al., 2018).

As in non-avialan dinosaurs and most stemward avialans (Hendrickx et al., 2015; Wang et al., 2022), the quadrate has a bicondylar mandibular process, and an orbital process that is dorsoventrally deep and broadly convex anteriorly (Fig. 6). In contrast, the orbital process is transformed into a pointed structure in crownward avialans such as *Ichthyornis* (Baumel and Witmer, 1993; Field et al., 2018). As in non-avialan paravians and *Archaeopteryx* (Elżanowski and Stidham, 2011; Hendrickx et al., 2015; Stidham and O'Connor, 2021), the anterior apex is near the dorsoventral midpoint of the orbital process (Fig. 6A, E), rather than being more ventrally located as in some Cretaceous avialans such as *Sapeornis* and *Yuanchuavis* (Hu et al., 2019; Wang et al., 2022). Like non-avialan dinosaurs and stemward avialans (e.g., *Archaeopteryx*, *Yuanchuavis*) (Norell et al., 2006; Hendrickx et al., 2015; Wang et al., 2022), the dorsal margin that extends from the orbital process to the otic process is straight. In contrast, that margin is deeply concave dorsally in most crownward avialans (Baumel and Witmer, 1993). As in early-diverging avialans, the single-headed otic process bears a low lateral ridge that extends down to the lateral condyle (Fig. 6A; Stidham and O'Connor, 2021; Wang et al., 2022). In contrast, in dromaeosaurids a prominent triangular process (Norell et al., 2006:fig. 10c) projects laterally from the otic process and contacts the squamosal and quadratojugal (Hendrickx et al., 2015; Xu et al., 2015). The posterior

surface of the quadrate shaft is not perforated by a foramen as in some troodontids such as *Troodon*, *Sinovenator* (Fig. 6C), and some enantiornithines (e.g., *Pengornis*) (Makovicky et al., 2003; O'Connor and Chiappe, 2011; Yin et al., 2018). The straight quadrate ridge extends anteroventrally (Fig. 6F), rather than being bowed anteriorly as in *Sinovenator* and *Parabohaiornis* (Yin et al., 2018; Wang, 2023). Like early avialans (Wang et al., 2021, 2022), the lateral and medial mandibular condyles are posteriorly located relative to the quadrate shaft, rather than being level with the latter as in non-avialan theropods (Hendrickx et al., 2015; Xu et al., 2015). As most non-avialan theropods (Hendrickx et al., 2015), the lateral condyle is larger than the medial one (Fig. 6D), opposite of the condition present in *Linheraptor*, *Archaeopteryx*, and some enantiornithines (O'Connor and Chiappe, 2011; Xu et al., 2015; Kundrát et al., 2019). The lateral condyle is more posteriorly and ventrally located relative to the medial condyle; whereas they are roughly co-planar in some non-avialan therapods (e.g., *Tsaagan*; Norell et al., 2006; Hendrickx et al., 2015), and the medial condyle is more posteriorly positioned in *Yuanchuavis* and *Jeholornis* (Hu et al., 2022; Wang et al., 2022). As in non-avialan and early avialan theropods (Hendrickx et al., 2015; Xu et al., 2015; Wang, 2023), a pterygoid condyle is absent, a derived feature that evolved later along the line to the crown birds (Wang et al., 2021, 2022).

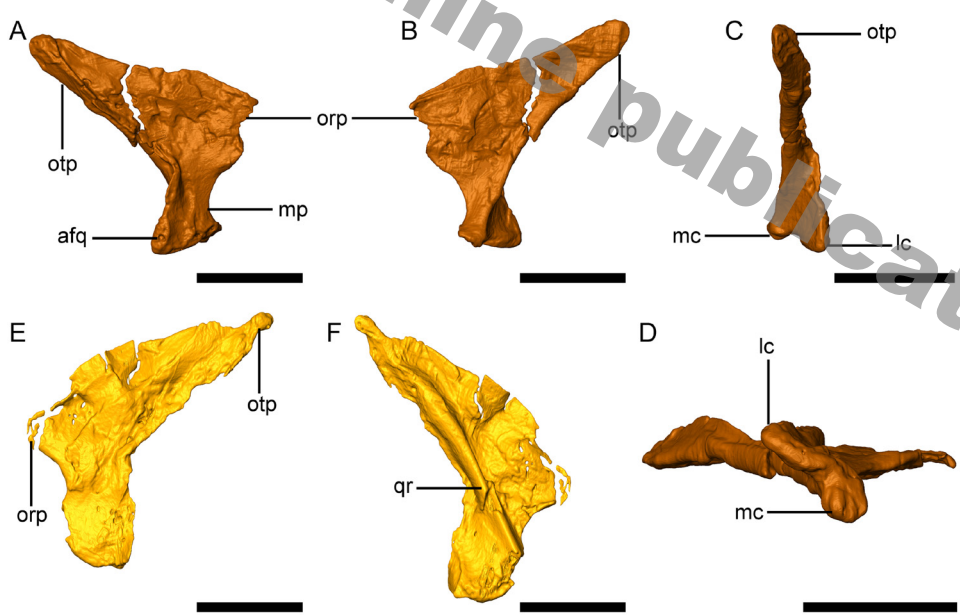

Fig. 6 Anatomy of the quadrate of *Anchiornis huxleyi* (STM 0-47) from Jianchang, Liaoning
A–D. right quadrate in lateral (A), medial (B), posterior (C), and ventral (D) views;
E, F. left quadrate in lateral (E) and medial (F) views
Abbreviations: afq. articular facet for quadratojugal; lc. lateral condyle; mc. medial condyle; mp. mandibular process; orp. orbital process; otp. otic process; qr. quadrate ridge. Scale bars = 5 mm

Morphology of the palatal elements remains obscure in *Anchiornis*, as well as many other Jurassic paravians. The pterygoid is the typical non-avialan maniraptoran condition in having a large quadrate ramus that projects far dorsal to the palatal surface in a position posterior to the orbit (Fig. 7A, B; Ostrom, 1969; Norell et al., 2006; Holliday and Witmer, 2008). This plesiomorphic condition is retained in stemward avialans such as enantiornithines (Wang et al., 2021). As in dromaeosaurids and enantiornithines (Ostrom, 1969; Wang et al., 2021, 2022), but unlike *Sinovenator* and *Jeholornis* (Yin et al., 2018; Hu et al., 2022), the quadrate ramus is forked posteriorly (Fig. 7A). An ectopterygoid wing, present in *Archaeopteryx* and some non-avian theropods (Elżanowski and Wellnhofer, 1996; Eddy and Clarke, 2011; Rauhut et al., 2018), is absent here as in *Sinovenator* and enantiornithines (Yin et al., 2018; Wang et al., 2021). The palatine ramus is as long as the quadrate ramus, whereas the former is twice longer than the latter in other non-avialan paravians and some early avialans (Yin et al., 2018; Wang et al., 2021; Hu et al., 2022). The pterygoid in *Anchiornis* is notably shorter than in other Mesozoic paravians. Specifically, the bone is slightly longer than the dorsoventral height of the quadrate in *Anchiornis*, whereas the pterygoid is substantially longer in other non-avialan theropods and early avialans (Ostrom, 1969; Yin et al., 2018; Wang et al., 2021, 2022; Hu et al., 2022). We suggest a short pterygoid as a diagnostic character of *Anchiornis*.

Like some dromaeosaurids such as *Velociraptor* (Ostrom, 1969; Barsbold and Osmólska, 1999), the tetraradiate palatine is mediolaterally broad (Fig. 7C, D), contrasting with the elongate and slender condition that is present in some troodontids (e.g., *Sinovenator*, *Gobipteryx*; Tsuihiji et al., 2014; Yin et al., 2018), *Archaeopteryx* and more crownward avialans (Elżanowski and Wellnhofer, 1996; Zusi and Livezey, 2006; Torres et al., 2021; Wang et al., 2022). As in dromaeosaurids and *Archaeopteryx* (Currie, 1995; Eddy and Clarke, 2011), the choanal process is hooked anteriorly, contrasting with both the medially oriented form, as in *Sapeornis* and *Yuanchuavis* (Hu et al., 2019; Wang et al., 2022), and the straight and anteriorly directed condition, as in *Sinovenator* and *Allosaurus* (Madsen, 1976; Yin et al., 2018). The pterygoid process is slightly longer than the choanal process, representing an intermediate stage from the ancestral therapod condition to the further elongate form in later-diverging avialans (Madsen, 1976; Elżanowski and Wellnhofer, 1996; Hu et al., 2019; Wang et al., 2022). The jugal process is present, a plesiomorphic condition for theropods (Zusi and Livezey, 2006; Wang et al., 2022). This structure is weakly developed in *Archaeopteryx* (Rauhut et al., 2018; but see Elżanowski and Wellnhofer, 1996) and is absent in other avialans (Torres et al., 2021; Wang et al., 2022). The maxillary process is proportionately shorter than in *Sinovenator* and early avialans such as *Archaeopteryx* and *Yuanchuavis*. As in dromaeosaurids (e.g., *Velociraptor* and *Dromaeosaurus*; Currie, 1995; Barsbold and Osmólska, 1999), the posterior margin of the internal naris (between the

choanal and maxillary processes) is parabolic, contrasting with the deeply notched condition that is present in *Sinovenator* and *Archaeopteryx* (Rauhut et al., 2018; Yin et al., 2018). The dorsal surface of the palatine bears three depressions at the base of the pterygoid and choanal processes and along the lateral margin, respectively, which are separated from one another by a triradiate embossment (Fig. 7C). This feature is absent in *Sinovenator*, *Deinonychus*, and early avialans such as *Archaeopteryx* and *Ichthyornis* (Ostrom, 1969; Rauhut et al., 2018; Yin et al., 2018; Torres et al., 2021). Unlike *Archaeopteryx* and *Deinonychus* (Ostrom, 1969; Rauhut et al., 2018), the lateral margin of the palatine is not thickened.

As in non-avialan theropods and *Archaeopteryx* (Currie, 1995; Elżanowski and Wellnhofer, 1996; Barsbold and Osmólska, 1999), the ectopterygoid has a posteriorly recurved jugal process (Fig. 7E, F), contrasting with the straight form observed in *Sapeornis* and *Yuanchuavis* (Wang et al., 2022). The lateral end of the jugal process is not expanded anteroposteriorly as in some non-avialan theropods (e.g., Allosaurs) and early avialans (e.g., *Yuanchuavis* and *Sapeornis*; Madsen, 1976; Godefroit et al., 2013; Wang et al., 2022). The jugal process terminates proximal to the midpoint of the pterygoid process, but it approaches the posterior margin of the pterygoid process in *Archaeopteryx* and some non-avialan theropods such as *Sinovenator* and dromaeosaurids (Currie, 1995; Elżanowski and Wellnhofer, 1996; Yin et al., 2018). The subtemporal fenestra defined by the jugal and pterygoid processes is relatively wider than in non-avialan theropods including *Sinovenator* and *Deinonychus* (Ostrom, 1969; Yin et al., 2018). Like some basal non-avialan theropods (e.g., *Sinoraptor*, *Allosaurus*) (Madsen, 1976; Currie and Zhao, 1993), the pterygoid flange is prominent and hooked posteriorly (Fig. 7E). In contrast, this flange is reduced in other paravians such as *Archaeopteryx* and some troodontids (Elżanowski and Wellnhofer, 1996; Tsuihiji et al., 2014; Yin et al., 2018). As in *Sinovenator* (Yin et al., 2018), the pterygoid process is rectangular, contrasting with the semicircular shape that is present in stemward avialans such as *Archaeopteryx* and *Yuanchuavis* (Elżanowski and Wellnhofer, 1996; Tsuihiji et al., 2014; Wang et al., 2022). The pterygoid process lacks both the ventral pocket that is present in other non-avialan theropods and *Archaeopteryx* (Currie, 1995; Rauhut et al., 2018), and the dorsal depressions that are present in *Sinovenator* and *Deinonychus* (Ostrom, 1969; Yin et al., 2018).

The basicranial elements are severely crushed, leaving only the parasphenoid rostrum identifiable. As in some non-avialan theropods and enantiornithine IVPP V12707 (Currie and Zhao, 1993; Wang et al., 2021), the ventral surface of the rostrum is concave (Fig. 7G), rather than being convex as in *Cratonavis*, *Parabohaiornis*, and the crown groups (Baumel and Witmer, 1993; Li et al., 2023). A spatulate element preserved adjacent to the left palatine is interpreted as the anterior part of the vomer (Figs. 3, 7H). If this is the case, the asymmetric shape of this element indicates that the paired vomers are not fused as in

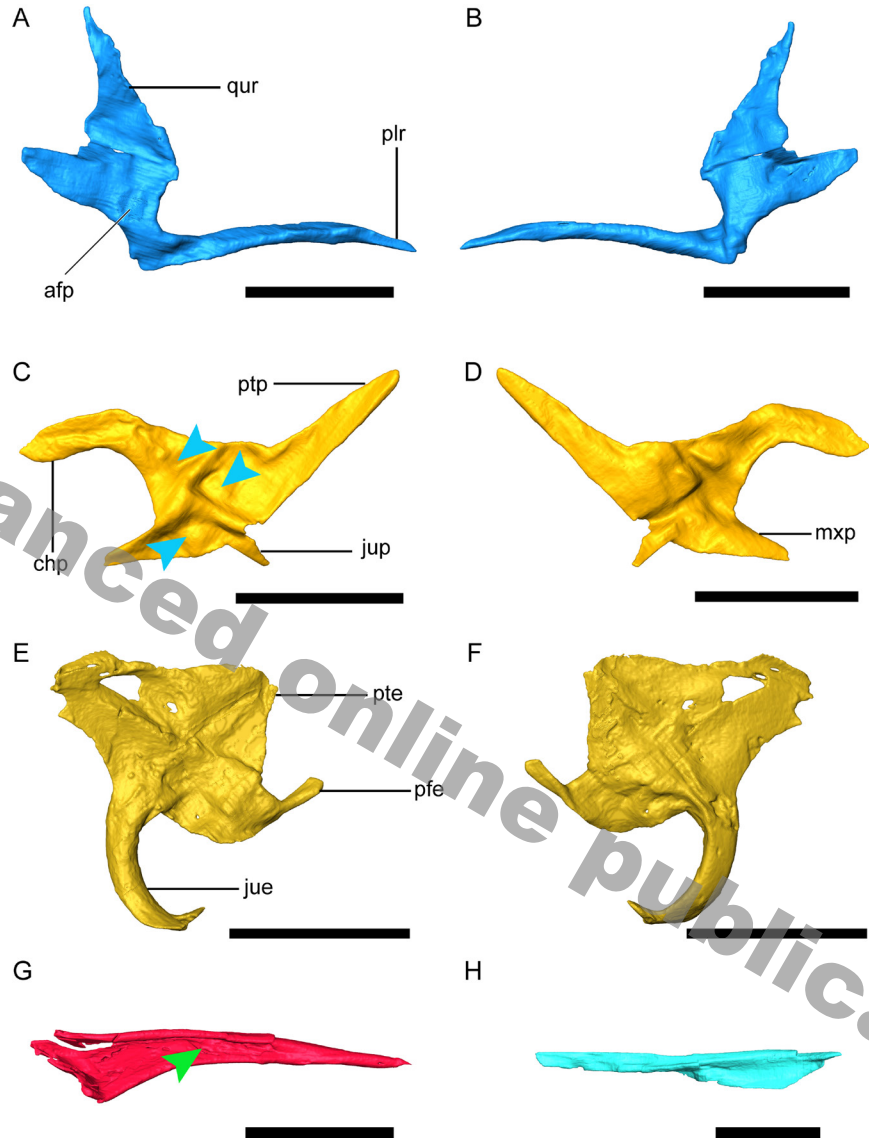

Fig. 7 Anatomy of the palatal elements of *Anchiornis huxleyi* (STM 0-47) from Jianchang, Liaoning

A, B. right pterygoid in medial (A) and lateral(B) views; C, D. left palatine in dorsal (C) and ventral (D) views; E, F. right ectopterygoid in dorsal (E) and ventral (F) views; G. parasphenoid rostrum in ventrolateral view; H. possible right vomer in dorsal view. The blue arrowheads in (C) denote the dorsal depressions, and the green arrowhead in (G) denotes the concave ventral surface of the parasphenoid rostrum

Abbreviations: afp. articular facet for basipterygoid process; chp. choanal process; jue. jugal process of ectopterygoid; jup. jugal process; mxp. maxillary process; pfe. pterygoid flange of ectopterygoid; plr. palatine ramus; pte. pterygoid process of ectopterygoid; ptp. pterygoid process of palatine; qur. quadrate ramus. Scale bars = 5 mm

some non-avialan and avialan theropods (e.g., *Archaeopteryx*, *Sapeornis*; Elżanowski and Wellnhofer, 1996; Hu et al., 2019).

As in many non-avialan theropods, the dentary is ventrally convex (Fig. 8A, B; Weishampel et al., 2004; Sullivan and Xu, 2017), which contrasts both with the dorsally convex condition, as in *Jeholornis* and *Sapeornis* (Hu et al., 2019, 2022), and the straight form, as in *Archaeopteryx* and some ornithothoracines (Elżanowski and Wellnhofer, 1996; O'Connor and Chiappe, 2011; Wang and Zhou, 2017). The lateral surface of the dentary bears a groove that widens posteriorly and houses nutritional foramina (Fig. 8B), a derived feature shared by *Anchiornis* and troodontids (Hu et al., 2009). Pei et al. (2017a) described that the dentary ended with a sheet-like posteroventral process. Although we cannot reexamine these specimens at first hand, the posterior end is only fully visible in the right dentary of PKUP V1068 in that study, and it is broken and compressed with other elements (Pei et al., 2017a:fig. 5). Our CT scanning show that both dentaries have a posteroventrally sloping posterior margin (Fig. 8A, B), as in other non-avialan theropods and some early-diverging avialans (O'Connor and Chiappe, 2011; Sullivan and Xu, 2017; Wang and Zhou, 2017). We posit that the "sheet-like" structure, reported in Pei et al. (2017a), in fact represents another element (e.g., prearticular, splenial?).

The teeth of STM 0-47 are complete and most of them remain *in situ*, enabling us to know the tooth count for the first time in *Anchiornis*. There are 4, 12, and 16 premaxillary, maxillary, and dentary teeth, respectively (Figs. 4A, B, 8A, B), which differ from previous estimation (Hu et al., 2009; Pei et al., 2017a). For instance, Hu et al. (2009) reconstructed 21 dentary teeth, but provided no direct evidence. The dentary tooth count is more than in many stemward avialans and dromaeosaurids (e.g., *Velociraptor* and *Tsaagan*; Barsbold and Osmólska, 1999; Norell et al., 2006; Wang and Zhou, 2017; Zhou et al., 2019), but fewer than in most troodontids (Makovicky and Norell, 2004; Norell et al., 2009). As in early avialans (Elżanowski and Wellnhofer, 1996; O'Connor and Chiappe, 2011; Zhou et al., 2019), the tooth crowns are recurved distally. Like dromaeosaurids and early avialans (Elżanowski and Wellnhofer, 1996; Norell and Makovicky, 2004; Rauhut et al., 2018), the premaxillary teeth are closely packed, and the maxillary and dentary teeth are relatively sparsely spaced. In contrast, troodontids are characteristically having closely packed anterior dentary teeth (Currie, 1987). The tooth row approaches the posterior end of the dentary, proportionately much longer than in many dromaeosaurids (Barsbold and Osmólska, 1999; Norell and Makovicky, 2004), troodontids (Tsuihiji et al., 2014; Xu et al., 2017), and stemward avialans (Rauhut et al., 2018; Zhou et al., 2019; Wang et al., 2022). Like dromaeosaurids and avialans (Turner et al., 2012; Wang and Zhou, 2017), the teeth are placed in individual socket, rather than being in a continuous groove as in troodontids (Fig. 8A; Currie, 1987). Contrary to Pei et al. (2017a), the interdentary plate is absent in STM 0-47

as in other paravians except *Archaeopteryx* (Currie, 1987; Elżanowski and Wellnhofer, 1996; Wang and Zhou, 2017). The anterior four dentary teeth are smaller and more recurved than the succeeding ones.

The triangular splenial lacks the foramen that is present in early avialans such as *Archaeopteryx* and *Pterygornis* (Fig. 8C; Rauhut et al., 2018; Wang et al., 2021). Unlike dromaeosaurids and troodontids (Makovicky and Norell, 2004; Norell and Makovicky, 2004), but as in early avialans (O'Connor and Chiappe, 2011; Turner et al., 2012), the bone is not visible laterally.

The surangular has a convex dorsal margin which thickens transversely close to the articular facet for the upper jaw (Fig. 8D–F). The angular is bowed ventrally and has an anterior process that curves dorsally and separates the dentary from the external mandibular fenestra (Fig. 8D), a diagnostic feature of the Deinonychosauria (Xu et al., 2017). The dorsal margin of the angular rises dorsally to form the posteroventrally margin of the external mandibular fenestra. As in other deinonychosaurs (Currie, 1995; Makovicky and Norell, 2004; Norell and Makovicky, 2004; Xu et al., 2015), but unlike early avialans except confuciusornithids (O'Connor and Chiappe, 2011; Wang and Zhou, 2017; Wang et al., 2022), the external mandibular fenestra is laterally exposed (contradicting Pei et al., 2017a). Like *Byronosaurus* and *Xiaotingia* (Makovicky et al., 2003; Xu et al., 2011), the surangular fenestra of *Anchiornis* is anteroposteriorly longer than dorsoventrally high, as inprevious reconstructions (Hu et al., 2009; Pei et al., 2017a).

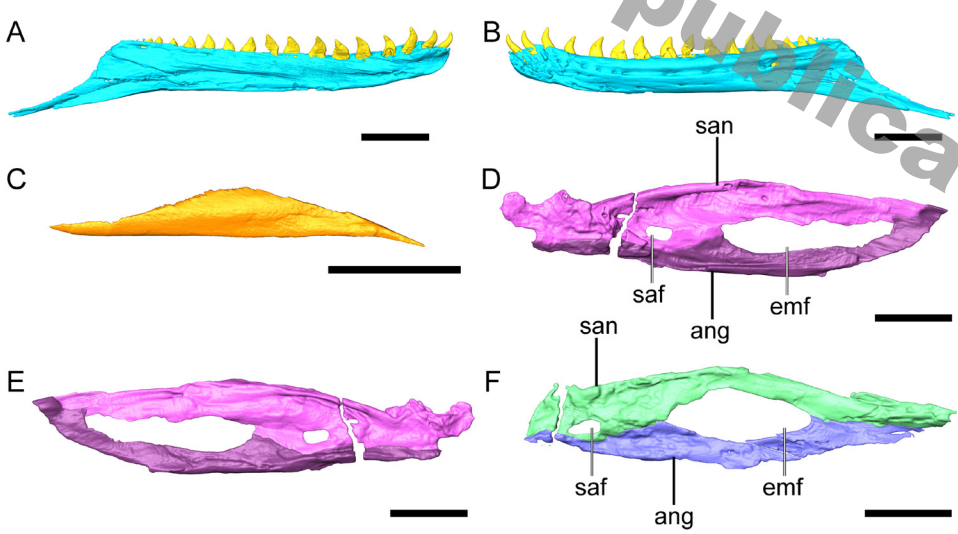

Fig. 8 Anatomy of the lower jaw elements of *Anchiornis huxleyi* (STM 0-47)
A, B. left dentary in medial (A) and lateral (B) views; C. left splenial in medial view; D, E. left post-dentary elements in medial (D) and lateral (E) views; F. right post-dentary elements in lateral view
Abbreviations: ang. angular; emf. external mandibular foramen; saf. surangular foramen; san. surangular
Scale bars = 5 mm

4 Discussion

The Jurassic paravians offer critical anatomical information to piece together the evolutionary acquisition of the bird "blueprint" (Xu et al., 2009, 2014; Brusatte et al., 2015), and *Anchiornis* stands out among Jurassic taxa given its wealthy fossil records and phylogenetic position (Zheng et al., 2018). Despite previous efforts attempting to comprehend the skeletal morphology of *Anchiornis* (Hu et al., 2009; Xu et al., 2009; Pei et al., 2017a), much remained unknown regarding its cranial anatomy, because of the two-dimensional preservation that severely limits the amount of data available. The gap in the knowledge of the cranial morphology impacts on our understanding about the phylogenetic affinity and functional anatomy of *Anchiornis*. The well-preserved skull of STM 0-47, visualized via high-resolution x-ray CT scanning, enables digital reconstruction of the cranial morphology of *Anchiornis* with great fidelity. Our study not only amends previous results, but more importantly demonstrates the three-dimensional configuration of some cranial elements for the first time. For instance, the following morphologies are revised for *Anchiornis*: the promaxillary fenestra is elliptical and is level with the maxillary fenestra in ventral extend (Fig. 4B); the lacrimal bears a recess at the juncture between the anterior and ventral processes (Fig. 4C); the jugal lacks the groove on its dorsomedial margin (Fig. 5D); the squamosal likely contacts the quadratojugal; the quadrate lacks the lateral flange (Fig. 6); the posterior end of the dentary slopes posteroventrally (Fig. 8A); the interdentary plates are absent (this structure appears variously present in other *Anchiornis* specimens, personal communication with Pei Rui) (Fig. 8A); and the external mandibular fenestra is laterally exposed (Fig. 8D–E).

Our digital reconstruction compensates a great deal of cranial morphology of *Anchiornis*, including the temporal and palatal regions that are reoevant to decipher the functional performance of this taxon (e.g., cranial kinesis). Specifically, the quadrate lacks the quadrate condyle (Fig. 6), indicating the absence of the condyle-based articulation between the quadrate and the pterygoid. Instead, the broad orbital process of the quadrate and the elongate quadrate ramus of the pterygoid reveal the presence of a scarf joint between the two elements, an ancestral dinosaurian condition retained by avialans stemward of ornithuromorphs (Holliday and Witmer, 2008; Wang et al., 2022). The tetraradiate palatine has a well-developed jugal process that forms a large articular facet for the jugal (Fig. 7C, D). The squamosal is morphologically more similar to that of *Archaeopteryx* than other paravians in having an anteriorly forked postorbital process, and a ventrally flexed paroccipital process (Fig. 5B). All these features combined with the complete postorbital bar show that *Anchiornis* preserves much of the ancestral dinosaurian condition in having a diapsid and almost akinetic skull, despite derived avialan-like features in postcranial regions.

This observation is in agreement with recent studies (Wang et al., 2021; Li et al., 2023), revealing that the skull was evolutionarily conservative along the line to early-diverging avialans.

The phylogenetic affinity of *Anchiornis* remains unsettled, with competing phylogenetic hypotheses that identify *Anchiornis* as avialan or troodontid (Hu et al., 2009; Xu et al., 2011; Turner et al., 2012; Agnolín and Novas, 2013; Pei et al., 2017a). On one hand, this controversy is ascribed to the sparse fossil record, which is further complicated by preservation that hinders direct observation (new analytical methods such as CT scanning can help resolve this issue). On the other hand, evolutionary mosaicism always impacts morphology-based phylogenetic inference. Previous studies show that the early evolution of avialans has been deeply shaped by mosaicism (Clarke and Middleton, 2008; Xu et al., 2014; Wang and Zhou, 2017), attesting to *Anchiornis* skull which exhibits mixed morphologies shared with dromaeosaurids, troodontids, and avialans. Although it is beyond the scope of this paper, we tentatively investigated to what degree the revised cranial anatomy could affect the phylogenetic position of *Anchiornis*, using the latest version of the Theropod Working Group matrix with modifications. 40 cranial character states of *Anchiornis* have been revised here. We performed maximum parsimony-based phylogenetic analyses using the same settings as in Xu et al. (2023) (see Materials and methods). The strict consensus tree is consistent with the previous result (Xu et al., 2023), in which *Anchiornis* was resolved in a polytomy that unites *Xiaotingia*, *Fujianvenator*, *Eosinopteryx*, and *Aurornis* (Fig. 9). This clade is poorly supported (Bootstrap value <50%; Bremer value = 0). The seemingly unchanged phylogentic topology is not surprising, considering that the revised cranial characters accounts <5% of the total characters. On the other hand, over 70% of the cranial characters in that data matrix cannot be determined for most other early-diverging paravians, which prevents comparison and offsets much phylogenetic significance introduced by revised cranial anatomy of *Anchiornis*. Therefore, much effort is needed to extract detailed and genuine cranial features of early-diverging paravians, particularly using techniques such as CT scanning, which together with discoveries of new fossils can help reconcile phylogenetic controversies of the earliest diverging avialans.

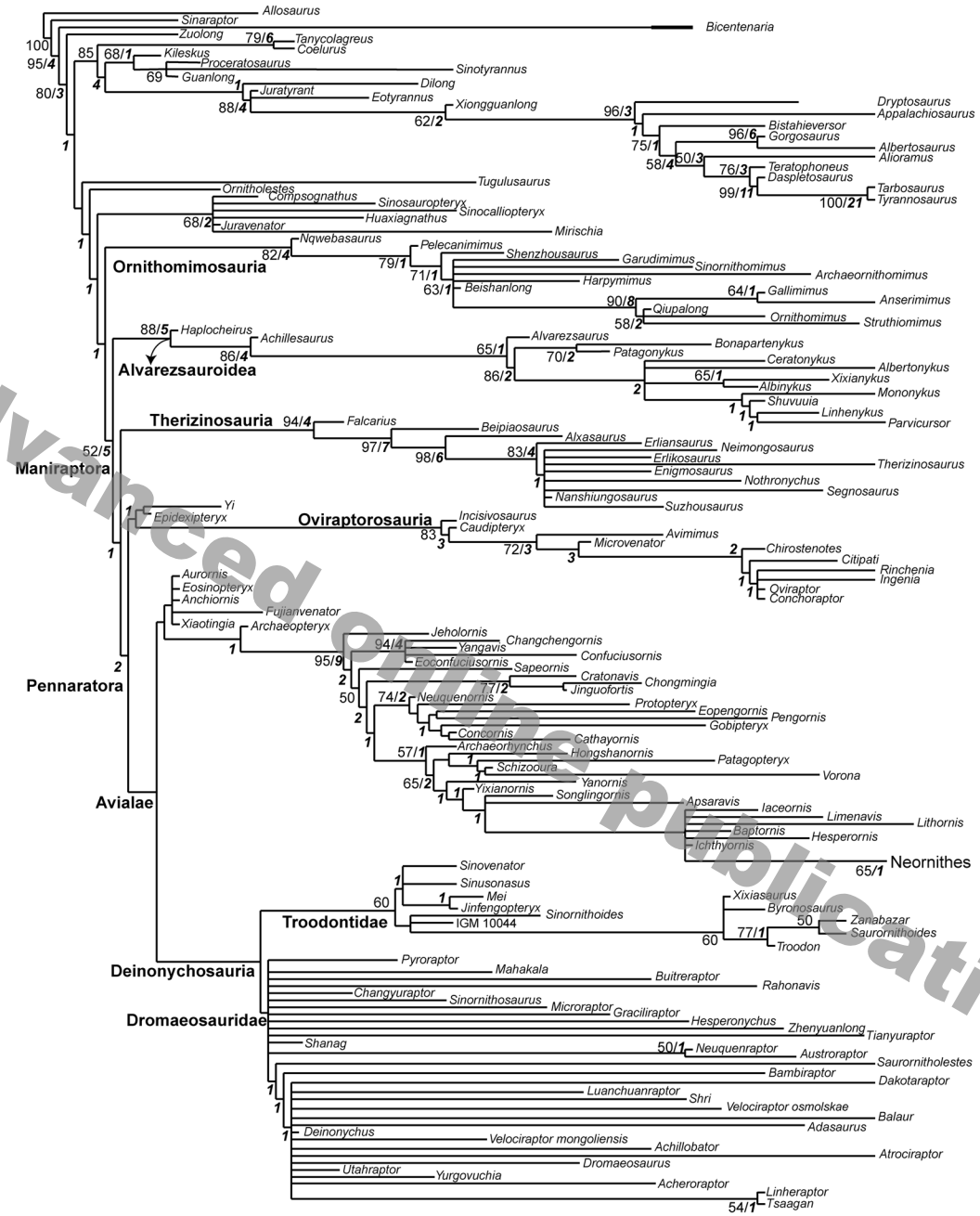

Fig. 9 Evolutionary tree showing the position of *Anchiornis*

The tree is the strict consensus derived from the phylogenetic analysis based on revised cranial characters of *Anchiornis*. The bootstrap and Bremer support values are indicated in normal and bold italic formats, respectively

Acknowledgements We thank YIN Pengfei, MIAO Song, and FENG Jiutong for helping in CT scanning. We thank Rui Pei and Fernando Novas for reviewing this manuscript. This research is supported by the National Natural Science Foundation of China (42225201), the Key Research Program of Frontier Sciences, CAS (ZDBS-LY-DQC002), the New Cornerstone Science Foundation through the XPLORER PRIZE, and Taishan Scholar Project of Shandong Province (Ts20190954).

赫氏近鸟龙(兽脚类恐龙：副鸟类)头骨形态对鸟类头骨演化的新启示

王 敏[1] 王孝理[2,3] 郑晓廷[2,3] 周忠和[1]

(1 中国科学院古脊椎动物与古人类研究所，中国科学院脊椎动物演化与人类起源重点实验室 北京 100044)

(2 临沂大学地质与古生物研究所 山东临沂 276005)

(3 山东省天宇自然博物馆 山东平邑 273300)

摘要：无论从何种维度，恐龙—鸟类的演化都是地球生命历史中最吸引人的一次演化事件，其中涉及大量形态学和生态学特征的改变。相较于头后骨骼形态，现有的研究对鸟类头骨的早期演化所取得的认识相对有限，这主要受限于保存较好的早期鸟翼类头骨化石材料的稀少。近鸟龙是目前已知最早的副鸟类(距今约1.6亿年)——副鸟类是指包含所有现代鸟类，但不包括尾羽龙类或者耀龙类的最广义类群。已知的近鸟龙类化石多达百余件，使得该类群成为研究非鸟兽脚类恐龙—鸟类演化过程中形态变化的最理想对象。然而目前有关近鸟龙类的头骨形态特征存在大量未知的内容。基于一件保存较好的近鸟龙类化石，详细描述了该类群头骨的形态结构，包括此前知之甚少的区域(例如颞区和颚区)。研究显示出近鸟龙保留了非鸟恐龙所具有的原始的双弓型非可动性的头骨形态。同时，近鸟龙头骨还呈现出与驰龙类、伤齿龙类，以及原始鸟翼类分别相似的局部形态特征，揭示了模块化演化深刻影响鸟翼类头骨的早期演化。

关键词：近鸟龙，鸟翼类，头骨，可动性，颚骨，鳞状骨

References

Agnolin F L, Novas F E, 2013. Avian Ancestors: A Review of the Phylogenetic Relationships of the Theropods Unenlagiidae, Microraptoria, *Anchiornis* and Scansoriopterygidae. Berlin: Springer-Verlag. 1–96

Barsbold R, Osmólska H, 1999. The skull of *Velociraptor* (Theropoda) from the late Cretaceous of Mongolia. Acta Palaeontol Pol, 44: 189–219

Baumel J J, Witmer L M, 1993. Osteologia. In: Baumel J J, King A S, Breazile J E et al. eds. Handbook of Avian Anatomy: Nomina Anatomica Avium, 2nd Ed. Cambridge: Nuttall Ornithological Club. 45–132

Brusatte S L, Lloyd G T, Wang S C et al., 2014. Gradual assembly of avian body plan culminated in rapid rates of evolution across the dinosaur-bird transition. Curr Biol, 24: 2386–2392

Brusatte S L, O'Connor J K, Jarvis E D, 2015. The origin and diversification of birds. Curr Biol, 25: R888–R898

Clarke J A, Middleton K M, 2008. Mosaicism, modules, and the evolution of birds: results from a Bayesian approach to the study of morphological evolution using discrete character data. Syst Biol, 57: 185–201

Currie P J, 1987. Bird-like characteristics of the jaws and teeth of troodontid theropods (Dinosauria, Saurischia). J Vert Paleont, 7: 72–81

Currie P J, 1995. New information on the anatomy and relationships of *Dromaeosaurus albertensis* (Dinosauria: Theropoda). J Vert Paleont, 15: 576–591

Currie P J, Zhao X, 1993. A new carnosaur (Dinosauria, Theropoda) from the Jurassic of Xinjiang, People's Republic of China. Can J Earth Sci, 30: 2037–2081

Eddy D R, Clarke J A, 2011. New information on the cranial anatomy of *Acrocanthosaurus atokensis* and its implications for the phylogeny of Allosauroidea (Dinosauria: Theropoda). PLoS One, 6: e17932

Elżanowski A, Stidham T A, 2011. A galloanserine quadrate from the Late Cretaceous Lance Formation of Wyoming. Auk, 128: 138–145

Elżanowski A, Wellnhofer P, 1996. Cranial morphology of *Archaeopteryx*: evidence from the seventh skeleton. J Vert Paleont, 16: 81–94

Field D J, Hanson M, Burnham D et al., 2018. Complete *Ichthyornis* skull illuminates mosaic assembly of the avian head. Nature, 557: 96–100

Godefroit P, Cau A, Hu D Y et al., 2013. A Jurassic avialan dinosaur from China resolves the early phylogenetic history of birds. Nature, 498: 359–362

Goloboff P A, Catalano S A, 2016. TNT version 1.5, including a full implementation of phylogenetic morphometrics. Cladistics, 32: 221–238

Hendrickx C, Araújo R, Mateus O, 2015. The non-avian theropod quadrate I: standardized terminology with an overview of the anatomy and function. PeerJ, 3: e1245

Holliday C M, Witmer L M, 2008. Cranial kinesis in dinosaurs: intracranial joints, protractor muscles, and their significance for cranial evolution and function in diapsids. J Vert Paleont, 28: 1073–1088

Hu D Y, Hou L H, Zhang L J et al., 2009. A pre-*Archaeopteryx* troodontid theropod from China with long feathers on the metatarsus. Nature, 461: 640–643

Hu H, Sansalone G, Wroe S et al., 2019. Evolution of the vomer and its implications for cranial kinesis in Paraves. Proc Natl Acad Sci USA, 116: 19571–19578

Hu H, Wang Y, Fabbri M et al., 2022. Cranial osteology and palaeobiology of the Early Cretaceous bird *Jeholornis prima* (Aves: Jeholornithiformes). Zool J Linn Soc, 198: 93–112

Kundrát M, Nudds J, Kear B P et al., 2019. The first specimen of *Archaeopteryx* from the Upper Jurassic Mörnsheim Formation of Germany. Hist Biol, 31: 3–63

Li Z H, Wang M, Stidham T A et al., 2023. Decoupling the skull and skeleton in a Cretaceous bird with unique appendicular morphologies. Nat Ecol Evol, 7: 20–31

Madsen J H, 1976. *Allosaurus fragilis*: a revised osteology. Utah Geol Min Surv Bull, 109: 1–163

Makovicky P J, Norell M A, 2004. Troodontidae. In: David B W, Peter D, Halszka O eds. The Dinosauria, 2nd Ed. Berkeley: University of California Press. 184–195

Makovicky P J, Norell M A, Clark J M et al., 2003. Osteology and relationships of *Byronosaurus jaffei* (Theropoda: Troodontidae). Am Mus Novit, 2003: 1–32

Mayr G, Pohl B, Peters D S, 2005. A well-preserved *Archaeopteryx* specimen with theropod features. Science, 310: 1483–1486

Norell M A, Makovicky P J, 2004. Dromaosauridae. In: David B W, Peter D, Halszka O eds. The Dinosauria, 2nd Ed. Berkeley: University of California Press. 196–209

Norell M A, Clark J M, Turner A H et al., 2006. A new dromaeosaurid theropod from Ukhaa Tolgod (Ömnögov, Mongolia). Am Mus Novit, 3545: 1–51

Norell M A, Makovicky P J, Bever G S et al., 2009. A review of the Mongolian Cretaceous dinosaur *saurornithoides* (Troodontidae: Theropoda). Am Mus Novit, 3654: 1–63

O'Connor J K, Chiappe L M, 2011. A revision of enantiornithine (Aves: Ornithothoraces) skull morphology. J Syst Palaeontol, 9: 135–157

Ostrom J H, 1969. Osteology of *Deinonychus antirrhopus*, an unusual theropod from the Lower Cretaceous of Montana. Bull Peabody Mus Nat Hist, 30: 1–165

Pei R, Li Q, Meng Q et al., 2017a. New specimens of *Anchiornis huxleyi* (Theropoda: Paraves) from the Late Jurassic of northeastern China. Bull Am Mus Nat Hist, 411: 1–67

Pei R, Norell M A, Barta D E et al., 2017b. Osteology of a new Late Cretaceous troodontid specimen from Ukhaa Tolgod, Ömnögovi Aimag, Mongolia. Am Mus Novit, 47: 1–47

Rauhut O W M, Foth C, 2020. The origin of birds: current consensus, controversy, and the occurrence of feathers. In: Foth C, Rauhut O W M eds. The Evolution of Feathers: From Their Origin to the Present. Cham: Springer International Publishing. 27–45

Rauhut O W M, Foth C, Tischlinger H, 2018. The oldest *Archaeopteryx* (Theropoda: Avialiae): a new specimen from the Kimmeridgian/Tithonian boundary of Schamhaupten, Bavaria. PeerJ, 6: e4191

Stidham T A, O'Connor J K, 2021. The evolutionary and functional implications of the unusual quadrate of *Longipteryx chaoyangensis* (Avialae: Enantiornithes) from the Cretaceous Jehol Biota of China. J Anat, 239: 1066–1074

Sullivan C, Xu X, 2017. Morphological diversity and evolution of the jugal in dinosaurs. Anat Rec, 300: 30–48

Torres C R, Norell M A, Clarke J A, 2021. Bird neurocranial and body mass evolution across the end-Cretaceous mass extinction: The avian brain shape left other dinosaurs behind. Sci Adv, 7: eabg7099

Tsuihiji T, Barsbold R, Watabe M et al., 2014. An exquisitely preserved troodontid theropod with new information on the palatal structure from the Upper Cretaceous of Mongolia. Naturwissenschaften, 101: 131–142

Turner A H, Makovicky P J, Norell M A, 2012. A review of dromaeosaurid systematics and paravian phylogeny. Bull Am Mus Nat Hist, 371: 1–206

Turner A H, Montanari S, Norell M A, 2021. A new dromaeosaurid from the Late Cretaceous Khulsan locality of Mongolia. Am Mus Novit, 2020: 1–48

Wang M, 2023. A new specimen of *Parabohaiornis martini* (Avialae: Enantiornithes) sheds light on early avian skull evolution. Vert PalAsiat, 61: 96–107

Wang M, Hu H, 2017. A comparative morphological study of the jugal and quadratojugal in early birds and their dinosaurian relatives. Anat Rec, 300: 62–75

Wang M, Zhou Z H, 2017. The evolution of birds with implications from new fossil evidences. In: Maina N J ed. The Biology of the Avian Respiratory System: Springer International Publishing. 1–26

Wang M, O'Connor J K, Zhou Z H, 2019. A taxonomical revision of the Confuciusornithiformes (Aves: Pygostylia). Vert PalAsiat, 57: 1–37

Wang M, Stidham T A, Li Z H et al., 2021. Cretaceous bird with dinosaur skull sheds light on avian cranial evolution. Nat Commun, 12: 3890

Wang M, Stidham T A, O'Connor J K et al., 2022. Insight into the evolutionary assemblage of cranial kinesis from a Cretaceous bird. eLife, 11: e81337

Weishampel B D, Dodson P, Osmólska H, 2004. The Dinosauria, 2ed Ed. Berkeley: University of California Press. 1–880

Xu L, Wang M, Chen R et al., 2023. A new avialan theropod from an emerging Jurassic terrestrial fauna. Nature, 621: 336–343

Xu X, Wu X, 2001. Cranial morphology of *Sinornithosaurus millenii* Xu et al. 1999 (Dinosauria: Theropoda: Dromaeosauridae) from the Yixian Formation of Liaoning, China. Can J Earth Sci, 38: 1739–1752

Xu X, Norell M A, Wang X et al., 2002. A basal troodontid from the Early Cretaceous of China. Nature, 415: 780–784

Xu X, Zhao Q, Norell M et al., 2009. A new feathered maniraptoran dinosaur fossil that fills a morphological gap in avian origin. Chinese Sci Bull, 54: 430–435

Xu X, You H L, Du K et al., 2011. An *Archaeopteryx*-like theropod from China and the origin of Avialae. Nature, 475: 465–470

Xu X, Zhou Z H, Dudley R et al., 2014. An integrative approach to understanding bird origins. Science, 346

Xu X, Pittman M, Sullivan C et al., 2015. The taxonomic status of the Late Cretaceous dromaeosaurid *Linheraptor exquisitus* and its implications for dromaeosaurid systematics. Vert PalAsiat, 53: 29–62

Xu X, Currie P, Pittman M et al., 2017. Mosaic evolution in an asymmetrically feathered troodontid dinosaur with transitional features. Nat Commun, 8: 14972

Yin Y, Pei R, Zhou C, 2018. Cranial morphology of *Sinovenator changii* (Theropoda: Troodontidae) on the new material from the Yixian Formation of western Liaoning, China. PeerJ, 6: e4977

Zheng X T, Wang X L, Sullivan C et al., 2018. Exceptional dinosaur fossils reveal early origin of avian-style digestion. Sci Rep, 8: 14217

Zhou Y C, Corwin S, Zhang F C, 2019. Negligible effect of tooth reduction on body mass in Mesozoic birds. Vert PalAsiat,

57: 38–50

Zhou Z H, 2004. The origin and early evolution of birds: discoveries, disputes, and perspectives from fossil evidence. Naturwissenschaften, 91: 455–471

Zhou Z H, Wang Y, 2017. Vertebrate assemblages of the Jurassic Yanliao Biota and the Early Cretaceous Jehol Biota: Comparisons and implications. Palaeoworld, 26: 241–252

Zusi R L, Livezey B C, 2006. Variation in the os palatinum and its structural relation to the palatum osseum of birds (Aves). Ann Carnegie Mus, 75: 137–180